Cenozoic high Sr/Y volcanic rocks in the Qiangtang terrane, northern Tibet: Geochemical and isotopic evidence for the origin of delaminated lower continental melts

Article *in* Geological Magazine · July 2008

DOI: 10.1017/S0016756808004548

Geol. Mag. **145** (*4*), *2008, pp. 463–474.* © *2008 Cambridge University Press*
doi:10.1017/S0016756808004548 *Printed in the United Kingdom*

Cenozoic high Sr/Y volcanic rocks in the Qiangtang terrane, northern Tibet: geochemical and isotopic evidence for the origin of delaminated lower continental melts

SHEN LIU*§, RUI-ZHONG HU*, CAI-XIA FENG*, HAI-BO ZOU†, CAI LI‡, XIAO-GUO CHI‡, JIAN-TANG PENG*, HONG ZHONG*, LIANG QI*, YOU-QIANG QI* &TAO WANG*

*State Key Laboratory of Ore Deposit Geochemistry, Institute of Geochemistry, Chinese Academy of Sciences, Guiyang 550002, China
†Department of Earth and Space Sciences, University of California, Los Angeles, CA 90095, USA
‡Department of Earth and Space Sciences, Jilin University, Changchun 130026, China

(*Received* 3 May 2007; *accepted* 23 July 2007; First published online 12 March 2008)

Abstract – Geochemical and Sr–Nd–Pb isotopic data are presented for volcanic rocks from Zougouyouchaco (30.5 Ma) and Dogai Coring (39.7 Ma) of the southern and middle Qiangtang block in northern Tibet. The volcanic rocks are high-K calc-alkaline trachyandesites and dacites, with SiO_2 contents ranging from 58.5 to 67.1 wt % The rocks are enriched in light REE (LREE) and contain high Sr (649 to 986 ppm) and relatively low Yb (0.8 to 1.2 ppm) and Y (9.5 to 16.6 ppm) contents, resulting in high La/Yb (29–58) and Sr/Y (43–92) ratios, as well as relatively high MgO contents and Mg no., similar to the compositions of adakites formed by slab melting in subduction zones. However, the adakitic rocks in the Qiangtang block are characterized by relatively low $\varepsilon_{Nd}(t)$ values (−3.8 to −5.0) and highly radiogenic Sr (($^{87}Sr/^{86}Sr)_i$ = 0.706–0.708), which are inconsistent with an origin by slab melting. The geochemistry and tectonics indicate that the adakitic volcanic rocks were most likely derived from partial melting of delaminated lower continental crust. As the pristine adakitic melts rose, they interacted with the surrounding mantle peridotite, elevating their MgO values and Mg numbers.

Keywords: adakitic rocks, lower crust, delamination, Cenozoic, Tibet.

1. Introduction

Post-collisional potassic volcanic rocks, following the late Cretaceous Indo-Asian collision (*c.* 70 Ma: Yin & Harrison, 2000), are widely distributed in the Lhasa, Qiangtang and Songpan–Ganzi blocks in the Tibetan Plateau (Coleman & Hodges, 1995; Turner *et al.* 1996; Chung *et al.* 1998; Williams *et al.* 2001; Ding *et al.* 2003, 2007). These ultrapotassic, potassic and high-potassium calc-alkaline series volcanic rocks (Deng, 1989, 1991, 1998; Liu, 1998) range in age from 65 Ma to < 1 Ma, and provide important information to help decipher the geological evolution of the Tibetan Plateau and the thermal and compositional structure of the lithosphere. Previous work (Deng, 1991; Arnaud *et al.* 1992; Turner *et al.* 1996; Ding *et al.* 1999; Miller *et al.* 1999; Hacker *et al.* 2000; Lai & Liu, 2001; Chung *et al.* 2003; Ding *et al.* 2003, 2007) indicates that these volcanic rocks exhibit negative Nb, Ta and Ti anomalies, strong enrichment in incompatible elements, and relatively radiogenic Sr and Pb and unradiogenic Nd isotopic ratios, suggesting that the parental magmas were derived from an enriched lithospheric mantle source that has been isolated from the convecting asthenosphere since at least Proterozoic time (e.g. Turner *et al.* 1996). However, it has been proposed that the parental magmas of some young lavas (0–3 Ma) were derived from a mafic granulitic or eclogitic lower-crustal source in thickened lower crust (Cooper *et al.* 2002). The rocks evolved from such parental magmas will have features similar to adakitic rocks formed by slab melting in terms of trace element composition (Atherton & Petford, 1993; Kay & Kay, 1993; Xu *et al.* 2002). Some of the potassic adakitic rocks in the Lhasa, northern Qiangtang and the Songpan–Ganzi terranes are now interpreted as partial melts of the lower crust (Chung *et al.* 2003; Hou *et al.* 2004; Lai, Qin & Li, 2007; Wang *et al.* 2005). Studies of Cenozoic adakitic rocks provide a good opportunity to investigate the thickening and foundering of lower continental crust beneath the Tibetan Plateau. However, little information exists on the adakitic rocks from the Qiangtang region. Here we report Nd, Sr, and Pb isotopic compositions and elemental concentrations of the volcanic rocks from two new localities (Zougouyouchaco and Dogai Coring) in the southern and middle Qiangtang region (Fig. 1), and compare our results with published data from post-collisional volcanic rocks from Qiangtang Terrane. Our objectives are: (1) to advance a better understanding of lower crustal magmatic processes of the Tibetan Plateau, (2) to report the newly discovered

§Author for correspondence: liushen@vip.gyig.ac.cn

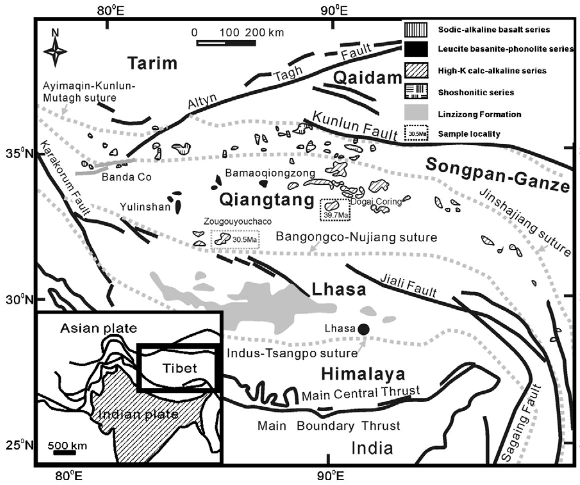

Figure 1. Map of the Tibetan Plateau showing the major terranes, the distribution of Cenozoic volcanic rocks and some of the main faults (modified from Yin & Harrison, 2000).

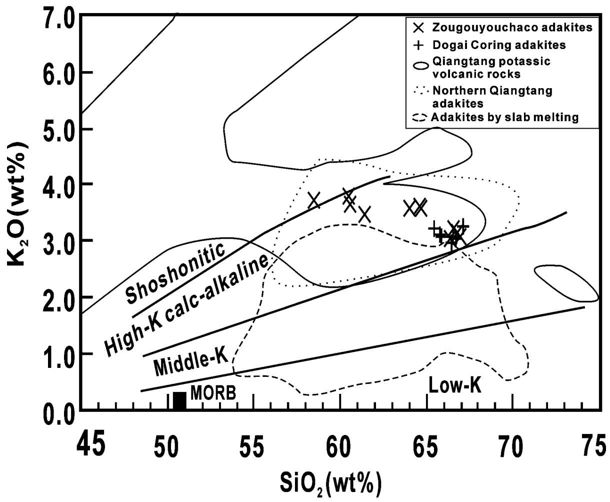

Figure 2. K_2O v. SiO_2 diagram of the Cenozoic volcanic rocks in northern Tibet. The Qiangtang potassic volcanic rocks are from Pearce & Houjun (1993); Turner *et al.* (1996); Deng (1998); Ding *et al.* (1999, 2003); Yin *et al.* (2004); Williams *et al.* (2004); Turner *et al.* (1996); Tan, Pan & Xu (2000); Lai & Liu (2001); Lai *et al.* (2006). Northern Qiangtang adakitic rocks are from Lai, Qin & Li (2007). Data field for adakites by slab melting is from published data (Defant & Drummond, 1990; Kay, Ramos & Marquez, 1993; Stern & Kilian, 1996, and references therein).

adakites in the northern Tibetan Plateau, and (3) to constrain their mechanism of formation.

2. Geological background and petrography

The Tibetan Plateau comprises six terranes, from south to north: Himalaya, Lhasa, Qiangtang, Songpan–Ganzi, Kunlun and Tarim (Fig. 1). The Tibetan Plateau has been created by collision of India–Asia since the early Cenozoic, about 55 Ma ago (Chung *et al.* 1998; Yin & Harrison, 2000). The Qiangtang terrane is bounded by the Jinshajiang (or Jinsha) suture to the north, and Bangong suture to the south (Fig. 1). It is generally accepted that suturing of the Songpan–Ganzi and Qiangtang terranes occurred in pre-Jurassic time (Tapponnier *et al.* 2001), and the Qiangtang terrane has been in an intra-continental setting since the Jurassic. Cenozoic lavas are widely distributed in the Qiangtang terrane (Pearce & Houjun, 1993; Turner *et al.* 1996; Deng, 1998; Tan, Pan & Xu, 2000; Lai & Liu, 2001; Ding *et al.* 1999, 2003;Yin *et al.* 2004; Williams *et al.* 2004; Lai *et al.* 2006), with ages from *c.* 65 Ma to *c.* 24 Ma, in three volcanic series: Na-rich alkaline basalt (65–40 Ma), leucite basanite–phonolite (29–24 Ma), and high-K calc-alkaline (40–29 Ma) (Chi *et al.* 1999). Samples for this study were collected from Zougouyouchaco and Dogai Coring, in the Qiangtang terrane (Fig. 1). ^{40}Ar–^{39}Ar ages of these rocks are 39.7 Ma (Dogai Coring) and 30.5 Ma (Zougouyouchaco: Chi *et al.* 1999; Li *et al.* 2006). In this paper, the ^{40}Ar–^{39}Ar ages for Zougouyouchaco and Dogai Coring are used for the age-correction of Nd, Sr and Pb isotopic compositions. Morphologically, the volcanic rocks are preserved as domes along with recent clastic alluvial deposits, suggesting subsequent tectonic uplift and erosion after eruption. The available data indicate that intermediate to acidic volcanic rocks are dominant in the Qiangtang area (Deng, 1998) (Fig. 2), whereas mafic volcanic rocks are common in the western Qiangtang terrane (Deng, 1998; Ding *et al.* 1999, 2003). The adakitic volcanic rocks discussed here include trachyandesites, trachydacites and dacites from Zougouyouchaco, and trachydacites and dacites from Dogai Coring. All of these samples are porphyritic. Dacites from Dogai Coring and Zougouyouchaco contain phenocrysts of quartz, oligoclase and minor orthopyroxene and biotite, and groundmass with felsophyric texture consisting of oligoclase, sanidine and quartz. Trachydacites from Zougouyouchaco and Dogai Coring have the same mineralogy as the dacites but exhibit a trachytic groundmass texture.

3. Analytical methods

Major elements were determined by PANalytical Axios-advance X-ray fluorescence spectrometer (XRF) at the State Key Laboratory of Ore Deposit Geochemistry, Institute of Geochemistry, Chinese Academy of Sciences (IGCAS), using fused lithum-tetraborate glass pellets. Analytical precision as determined on the Chinese National Standard GSR-1 was generally around 1–5 % (Table 1). Loss on ignition was obtained by weighing after 3 hours of combustion at 950 °C.

The trace elements were analysed using a Finnigan MAT ELEMENT inductively coupled plasma source mass spectrometer (ICP-MS) at the IGCAS, following procedures described by Qi, Hu & Gregoire (2000). Rh was used as an internal standard to monitor signal drift during counting. The international standards GBPG-1

Table 1. Major oxides (wt %) of the volcanic rocks in Qiangtang, northern Tibet

Sample	Sample locality	Rock types	SiO_2	TiO_2	Al_2O_3	FeOT	MnO	MgO	CaO	Na_2O	K_2O	P_2O_5	LOI	Total	Mg no.	FeO_T/MgO
ZGYC-01	Zougouyouchaco	Trachydacite	63.99	0.9	15.64	4.29	0.06	1.92	3.93	4.37	3.58	0.36	0.64	99.68	45	2.2
ZGYC-02	Zougouyouchaco	Trachyandesite	60.52	1.04	15.09	4.82	0.07	2.69	5.15	3.84	3.81	0.5	1.99	99.52	50	1.8
ZGYC-03	Zougouyouchaco	Trachyandesite	61.43	0.85	15.28	4.25	0.06	2.45	5.15	4.03	3.48	0.35	1.91	99.24	51	1.7
ZGYC-04	Zougouyouchaco	Trachyandesite	60.58	0.98	15.30	4.50	0.07	2.92	5.12	3.67	3.66	0.44	2.16	99.40	54	1.5
ZGYC-05	Zougouyouchaco	Trachyandesite	58.48	1.01	15.43	5.50	0.07	2.65	5.02	4.22	3.73	0.51	2.07	98.69	46	2.1
ZGYC-06	Zougouyouchaco	Trachydacite	64.58	0.87	15.38	4.12	0.05	1.89	3.64	4.26	3.61	0.35	0.79	99.54	45	2.2
ZGYC-07	Zougouyouchaco	Dacite	64.72	0.68	15.29	3.91	0.06	1.93	3.35	3.98	3.59	0.33	1.53	99.37	47	2.0
ZGYC-08	Zougouyouchaco	Dacite	66.93	0.48	15.38	3.74	0.05	1.85	3.29	4.12	3.08	0.15	0.55	99.62	47	2.0
ZGYC-09	Zougouyouchaco	Dacite	66.39	0.57	15.17	3.76	0.06	1.96	3.38	3.93	3.05	0.22	0.87	99.36	48	1.9
ZGYC-10	Zougouyouchaco	Trachydacite	66.83	0.49	15.26	3.12	0.06	1.91	2.86	4.23	3.16	0.17	1.24	99.33	52	1.6
DGC-01	Dogai Coring	Dacite	67.11	0.47	15.62	2.59	0.06	1.73	3.65	4.36	3.28	0.21	0.71	99.79	55	1.5
DGC-02	Dogai Coring	Dacite	65.75	0.42	15.43	3.74	0.05	1.54	3.37	4.34	3.12	0.16	1.64	99.56	43	2.4
DGC-03	Dogai Coring	Dacite	65.45	0.48	16.19	3.54	0.06	1.96	3.25	4.11	3.23	0.17	0.95	99.39	50	1.8
DGC-04	Dogai Coring	Dacite	66.46	0.47	15.87	3.43	0.05	1.92	2.89	4.60	2.97	0.17	0.73	99.56	50	1.8
DGC-05	Dogai Coring	Trachydacite	65.89	0.46	15.76	3.50	0.06	1.76	2.73	4.66	3.08	0.17	1.48	99.55	48	2.0
DGC-06	Dogai Coring	Dacite	66.52	0.45	15.51	3.32	0.06	2.12	3.49	4.24	3.07	0.16	0.92	99.86	53	1.6
DGC-07	Dogai Coring	Dacite	66.58	0.57	15.65	3.28	0.05	2.08	3.36	3.98	3.25	0.17	0.73	99.70	53	1.6
DGC-08	Dogai Coring	Dacite	66.7	0.55	15.47	3.21	0.05	1.94	3.43	4.04	3.05	0.18	0.66	99.28	52	1.7
GSR1		This study	72.69	0.28	13.47	2.15	0.06	0.41	1.51	3.26	5.01	0.1	0.78	99.72		
RV*		Recommended values	72.83	0.29	13.4	2.14	0.06	0.42	1.55	3.13	5.01	0.09	0.76	99.68		

LOI = Loss on Ignition, Mg no. = 100 × Mg/(Mg+ΣFe)

and OU-6 were used for analytical quality control (Table 2). The analytical precision is generally better than 5 % for trace elements.

Sr and Nd isotopes were measured by a Micromass Isoprobe multicollector inductively coupled plasma mass spectrometry (MC-ICPMS) at Guangzhou Institute of Geochemistry, Chinese Academy of Sciences (GIGCAS). Measured Sr and Nd isotopic ratios were normalized to $^{86}Sr/^{88}Sr = 0.1194$ and $^{146}Nd/^{144}Nd = 0.7219$, respectively. The measured Nd and Sr isotope standard values are $^{143}Nd/^{144}Nd = 0.512124 \pm 11$ (2σ) for Shin Etou and $^{87}Sr/^{86}Sr = 0.710243 \pm 14$ (2σ) for NBS987. The detailed analytical procedures for Sr and Nd isotope measurement have been documented elsewhere (Liang *et al.* 2003).

Samples for Pb isotope analyses were dissolved using a HF + $HClO_4$ mixture. Pb was extracted and purified using HBr and HCl anion microcolumn procedures. The Pb isotopes were determined using a MAT261 thermal ionization mass spectrometer at the Isotope Analysis Center of the Institute of Geology, Beijing Nuclear Industry. Pb isotopic ratios in samples have been corrected by reference to the analyses of NBS981 standard. Mass fractionation correction is 0.1 % per atomic mass unit for $^{206}Pb/^{204}Pb$, $^{207}Pb/^{204}Pb$ and $^{208}Pb/^{204}Pb$. Procedural blanks were < 100 pg for Nd, < 1 ng for Sr, and < 500 pg for Pb.

4. Analytical results

4.a. Major and trace elements

Major and trace element concentrations are given in Tables 1 and 2. The Zougouyouchaco and Dogai Coring volcanic rocks are classified as high-K calc-alkaline andesites and dacites (Fig. 2). They have high SiO_2 (58.5–67.1 wt %), Al_2O_3 (15.1–15.9 wt %), K_2O (2.97–3.81 wt %), Na_2O (> 3.6 wt %, K_2O/Na_2O < 1.0), high Sr (650–890 ppm), and low HREE and Y contents (Yb: 0.8–1.2 ppm; Y: 9–17 ppm). They also display elevated Sr/Y (43–92) and La/Yb (29–58) ratios (Fig. 3a, b). Furthermore, the volcanic rocks exhibit relatively low FeO_T/MgO (1.5–2.4) ratios and Yb contents, relatively high MgO (1.54–2.92 wt %), Mg no. (43–54), Cr (47.4–72.3 ppm) and Ni (37.5–64.7 ppm) contents (Figs 3b, 4a–h, 5; Tables 1, 2). In chondrite-normalized rare earth element (REE) diagrams, and in N-MORB normalized trace element diagrams (Fig. 6a, b), the volcanic rocks display significantly enriched light REE, strongly depleted heavy REE and no obvious Eu anomalies (Fig. 6a). They are strongly depleted in high field strength elements(HFSE)(Nb, Ta, and Ti), and relatively enriched in Rb, Th, La and Gd (Fig. 6b).

4.b. Sr, Nd and Pb isotope systematics

The Nd and Sr isotopic compositions of the volcanic rocks are characterized by high $^{87}Sr/^{86}Sr$ (0.7061–0.7077) and low $^{143}Nd/^{144}Nd$ (0.51233–0.51243) and thus negative $\varepsilon_{Nd}(t)$ values (−3.8 to −5.0) (Table 3; Fig. 7). The volcanic rocks also display highly radiogenic Pb isotopic compositions (Table 3). $^{207}Pb/^{204}Pb$ (15.895–16.031) and $^{208}Pb/^{204}Pb$ (39.411–39.786) in the rocks are unusually radiogenic and yield steep arrays that plot well above the Northern Hemisphere Reference Line (NHRL) (Hart, 1984), parallel to, but shifted to higher values of $^{206}Pb/^{204}Pb$ (18.928–19.046) than the Geochron (4.55 Ga) (Fig. 8). Steep

Table 2. Trace elements (ppm) of the volcanic rocks in Qiangtang, northern Tibet

Sample	Ba	Rb	Sr	Y	Zr	Nb	Th	Ni	V	Cr	Hf	Ta	U	Pb	Sc	Th/U	Rb/Ba	Th/Ba	La	Ce	Pr	Nd	Sm	Eu	Gd	Tb	Dy	Ho	Er	Tm	Yb	Lu	Eu/Eu*	(La/Yb)N	Sr/Y	Th/Ce
ZGYC-01	858	120	649	15.0	336	20.1	18.7	42.8	80.0	50.7	9.7	1.2	3.0	24.7	10.0	6.2	0.14	0.02	71.7	128	13.4	45.1	6.8	1.5	4.6	0.6	3.0	0.5	1.4	0.2	1.2	0.2	0.84	42	43	0.15
ZGYC-02	838	99.4	775	16.6	317	21.9	14.6	64.7	90.2	72.3	9.2	1.3	2.5	19.5	10.0	5.9	0.12	0.02	70.9	125	14.0	47.8	7.4	1.8	5.2	0.6	3.3	0.6	1.5	0.2	1.2	0.2	0.87	40	47	0.12
ZGYC-03	930	111	818	15.0	319	18.5	18.0	56.5	78.0	61.0	9.3	1.1	4.3	23.1	10.0	4.2	0.12	0.02	71.3	122	13.5	45.1	6.8	1.7	4.5	0.6	2.9	0.5	1.3	0.2	1.1	0.1	0.81	44	55	0.15
ZGYC-04	801	25.8	809	9.5	303	19.4	12.7	60.9	82.0	65.1	8.9	1.2	3.3	20.2	10.1	3.8	0.03	0.02	41.3	106	9.7	35.4	5.2	1.3	3.7	0.5	2.5	0.4	1.1	0.2	1.0	0.1	0.84	29	85	0.12
ZGYC-05	813	78.0	739	16.0	311	21.5	12.7	43.4	88.0	52.0	9.0	1.3	2.1	20.0	10.1	6.2	0.10	0.02	66.1	122	13.1	45.1	7.0	1.7	4.8	0.6	3.2	0.5	1.5	0.2	1.2	0.2	0.91	38	46	0.10
ZGYC-06	753	97.6	901	10.2	284	16.5	17.3	54.2	82.6	64.8	8.1	0.9	3.8	21.2	10.1	4.6	0.13	0.02	45.7	76.1	8.5	30.4	4.5	1.2	3.2	0.4	2.1	0.4	0.9	0.14	0.8	0.14	0.97	39	88	0.23
ZGYC-07	815	85.4	874	9.8	295	20.1	16.4	43.7	81.6	52.2	8.7	1.0	3.7	23.5	10.0	4.4	0.10	0.02	55.8	93.2	10.4	35.9	5.2	1.3	3.4	0.4	2.0	0.4	0.9	0.13	0.9	0.13	0.95	42	89	0.18
ZGYC-08	768	99.8	903	10.3	307	18.9	17.6	48.4	76.4	59.1	9.1	1.2	3.4	22.9	10.2	5.2	0.13	0.02	66.7	111	12.3	42.4	6.1	1.5	3.9	0.5	2.3	0.5	1.0	0.13	0.8	0.14	0.94	56	88	0.16
ZGYC-09	833	83.2	930	11.5	333	17.9	14.8	54.5	86.6	62.4	8.5	0.8	3.5	19.8	10.3	4.2	0.10	0.02	69.2	115	12.9	44.5	6.5	1.6	4.2	0.5	2.5	0.5	0.9	0.14	0.8	0.14	0.94	58	81	0.13
ZGYC-10	747	88.8	944	12.2	338	19.4	13.9	49.2	80.7	57.8	9.4	1.1	4.6	21.7	10.4	3.0	0.12	0.02	72.1	122	13.6	46.9	6.7	1.6	4.2	0.5	2.6	0.5	1.0	0.13	0.9	0.14	0.92	54	77	0.11
DGC-01	869	101	893	10.2	254	7.2	18.9	45.8	63.3	54.2	7.9	0.6	3.7	43.3	10.3	5.1	0.12	0.02	58.2	97.1	10.8	38.6	5.6	1.4	3.7	0.5	2.4	0.5	0.9	0.13	0.9	0.13	0.94	44	88	0.19
DGC-02	928	97.6	918	10.0	268	7.1	18.1	55.6	58.7	67.3	8.3	0.7	4.1	34.8	10.2	4.4	0.11	0.02	61.5	102	11.3	40.4	5.9	1.5	3.8	0.5	2.4	0.4	0.9	0.14	0.8	0.14	0.97	52	92	0.18
DGC-03	792	94	909	10.1	235	7.0	17.4	37.5	58.2	55.6	7.5	0.5	3.5	37.7	10.3	5.0	0.12	0.02	47.3	78.9	8.8	31.3	4.6	1.2	3.1	0.4	2.0	0.4	1.0	0.13	0.8	0.12	0.97	40	90	0.22
DGC-04	889	92.7	792	9.8	249	6.9	16.9	44.4	64.5	58.6	8.1	0.6	3.3	44.1	10.0	5.1	0.10	0.02	67.5	113	12.6	43.4	6.2	1.5	3.9	0.5	2.4	0.5	0.9	0.13	0.9	0.13	0.93	51	81	0.15
DGC-05	973	114	986	11.4	302	7.5	19.6	45.4	67.5	52.5	8.2	0.7	4.4	41.7	10.7	4.5	0.12	0.02	64.5	108	11.8	42.2	6.0	1.4	3.6	0.5	2.3	0.5	0.8	0.14	0.8	0.13	0.92	54	86	0.18
DGC-06	874	99.8	939	10.2	288	7.2	17.9	37.7	55.6	47.4	8.5	0.5	3.8	40.2	9.9	4.7	0.11	0.02	55.4	92.3	10.3	36.8	5.3	1.3	3.4	0.4	1.9	0.4	0.9	0.13	0.8	0.12	0.93	47	92	0.19
DGC-07	1262	90.0	885	10.0	220	7.1	18.8	43.6	61.0	57.3	7.6	0.5	3.6	29.6	10.2	5.3	0.07	0.01	54.1	90.0	10.0	35.0	5.1	1.2	3.2	0.4	2.0	0.3	0.9	0.1	0.8	0.1	0.93	45	89	0.21
DGC-08	1289	85.0	842	10.0	224	7.0	17.5	46.1	61.0	59.0	7.7	0.5	3.4	40.1	10.2	5.2	0.07	0.01	49.8	91.8	9.1	32.3	4.6	1.2	3.1	0.4	1.9	0.3	0.9	0.1	0.8	0.1	0.94	41	84	0.19
GBPG-1	910	54.7	364	17.3	232	9.7	11.2	61	97.0	179.0	5.9	0.41	0.8	14.6	13.9				51.9	102	11.3	43.6	6.7	1.8	4.73	0.58	3.27	0.68	1.97	0.32	2.01	0.31				
RV*	886	55.8	362	16.9	231	9.8	11.6	59.2	96.7	180	6.2	0.4	0.94	15.4	14.2				53	100	11.5	42	6.8	1.78	4.6	0.59	3.3	0.69	2.04	0.33	2.02	0.3				
OU-6	480	121	132	27.8	174	14.5	11.3	40.2	130	70.7	4.7	1.02	1.92	28.8	22.1				33.2	77.1	7.91	30.2	6.01	1.36	5.3	0.86	5.06	1.04	2.93	0.45	2.98	0.45				
RV*	471	123	129	26.1	168	14.2	11.2	38.5	131	71.2	4.72	1	1.93	27.9	21.9				32.6	77.6	7.78	30.4	5.98	1.38	5.35	0.87	5.03	1.04	2.94	0.46	2.95	0.46				

$Eu/Eu^* = Eu_N/(Sm_N+Gd_N)^{1/2}$; N – chondrite-normalized.

Table 3. Sr–Nd–Pb isotopic ratios of the volcanic rocks in Qiangtang, northern Tibet

Sample	$^{87}Rb/^{86}Sr$	$^{87}Sr/^{86}Sr$	2σ	$(^{87}Sr/^{86}Sr)_i$	$^{147}Sm/^{144}Nd$	$^{143}Nd/^{144}Nd$	2σ	$(^{143}Nd/^{144}Nd)_i$	$\varepsilon_{Nd}(t)$	$^{208}Pb/^{204}Pb$	$^{207}Pb/^{204}Pb$	$^{206}Pb/^{204}Pb$	$(^{208}Pb/^{204}Pb)_i$	$(^{207}Pb/^{204}Pb)_i$	$(^{206}Pb/^{204}Pb)_i$
ZGYC-01	0.9255	0.706804	10	0.706565	0.0874	0.512416	7	0.512398	−4.3	39.583	15.923	19.012	39.506	15.921	18.974
ZGYC-02	0.6515	0.706280	10	0.706114	0.0906	0.512399	5	0.512380	−4.7	39.640	15.979	19.052	39.564	15.977	19.012
ZGYC-04	0.5376	0.706295	6	0.706254	0.0885	0.512443	6	0.512425	−3.8	39.773	16.019	19.079	39.759	16.017	19.028
ZGYC-05	0.6440	0.706233	13	0.706097	0.0899	0.512429	7	0.512410	−4.1	39.611	15.972	19.034	39.546	15.970	19.001
ZGYC-06	0.3131	0.706624	13	0.706624	0.0895	0.512381	7	0.512363	−4.6	39.792	15.984	19.059	39.709	15.981	19.003
ZGYC-07	0.2824	0.706541	14	0.706541	0.0876	0.512372	8	0.512355	−4.8	39.657	15.962	19.029	39.586	15.960	18.980
ZGYC-08	0.3194	0.706587	10	0.706587	0.0870	0.512375	8	0.512358	−4.7	39.564	15.977	19.037	39.486	15.975	18.991
ZGYC-09	0.2585	0.706557	13	0.706557	0.0883	0.512364	6	0.512346	−4.9	39.487	15.898	18.983	39.411	15.895	18.928
ZGYC-10	0.2719	0.706589	14	0.706589	0.0864	0.512366	8	0.512349	−4.9	39.528	15.959	19.021	39.463	15.956	18.955
DGC-01	0.3269	0.706953	10	0.706953	0.0877	0.512363	6	0.512340	−4.8	39.781	15.982	19.056	39.723	15.980	19.021
DGC-02	0.3073	0.707245	14	0.707245	0.0883	0.512368	7	0.512345	−4.7	39.694	15.979	19.045	39.625	15.977	18.997
DGC-03	0.2989	0.707532	13	0.707532	0.0888	0.512358	6	0.512335	−4.9	39.813	16.026	19.079	39.752	16.024	19.041
DGC-04	0.3383	0.707611	14	0.707611	0.0864	0.512353	7	0.512331	−5.0	39.759	15.986	19.061	39.708	15.985	19.031
DGC-05	0.3341	0.707693	10	0.707693	0.0859	0.512361	6	0.512339	−4.8	39.805	15.993	19.068	39.742	15.991	19.025
DGC-06	0.3072	0.707143	10	0.707143	0.0871	0.512359	8	0.512336	−4.9	39.723	15.981	19.054	39.664	15.979	19.016
DGC-07	0.5343	0.707874	10	0.707704	0.0891	0.512364	7	0.512342	−4.8	39.844	16.033	19.080	39.786	16.031	19.046

Chondrite Uniform Reservoir (CHUR) values ($^{87}Rb/^{86}Sr = 0.0847$, $^{87}Sr/^{86}Sr = 0.7045$, $^{147}Sm/^{144}Nd = 0.1967$ $^{143}Nd/^{144}Nd = 0.512638$) are used for the calculation. $\lambda_{Rb} = 1.42\times10^{-11}$ year^{-1} (Steiger & Jäger, 1977); $\lambda_{Sm} = 6.54\times10^{-12}$ year^{-1} (Lugmair & Harti, 1978).

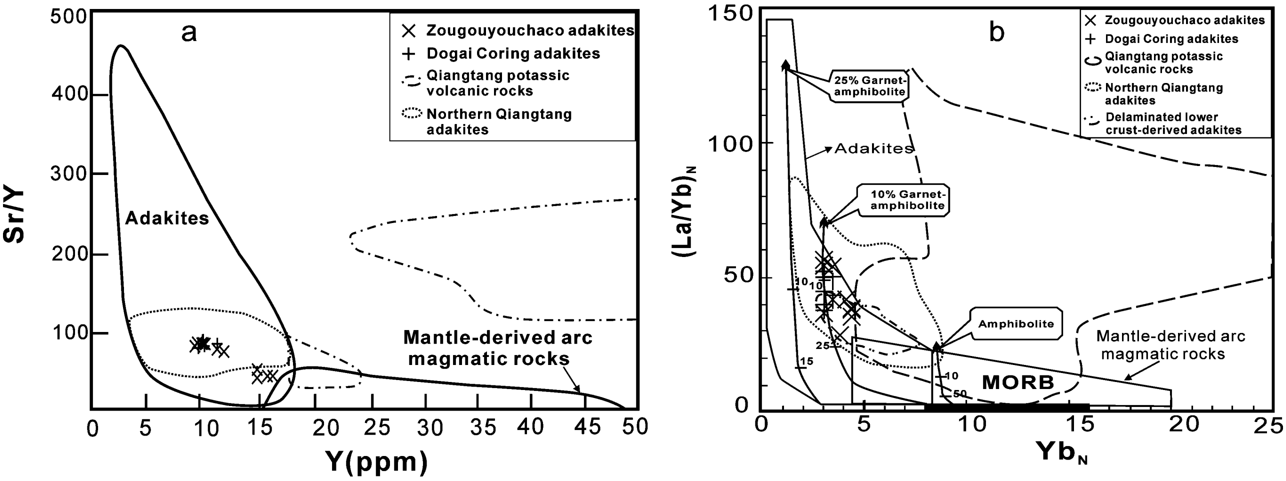

Figure 3. (a) Sr/Y v. Y and (b) $(La/Yb)_N$ v. Yb_N diagrams (Defant & Drummond, 1990) of the high-K calc-alkaline adakitic lavas from Qiangtang terrane, northern Tibet. Data for delaminated lower crust-derived adakitic rocks are from Xu *et al.* (2002) and Wang *et al.* (2004*a*,*b*, 2006). Other data sources are same as in Figure 2.

linear correlations between Pb isotopic ratios have been reported by previous researchers for other Tibetan lavas (Arnaud *et al.* 1992; Turner *et al.* 1996; Miller *et al.* 1999; Ding *et al.* 2003; Williams *et al.* 2004). The more variable $^{207}Pb/^{204}Pb$ and $^{208}Pb/^{204}Pb$ are interpreted to be a characteristic of Tibetan potassic lavas.

5. Discussion

5.a. Petrogenesis

5.a.1. Genetic model

The post-collisional potassic rocks of the Qiangtang terrane possess consistent chemical compositions (Figs 4, 7, 9). However, in contrast to many of the Qiangtang potassic rocks, the volcanic rocks in this study have high K_2O (2.97–3.81 wt %) and belong to the high-K calc-alkaline series (Table 1; Fig. 2). Furthermore, the high Sr and low HREE and Y contents (Tables 1, 2) result in elevated Sr/Y (43–92) and La/Yb (29–58) ratios, characteristic of typical adakites (Fig. 3a, b). Discussing the genesis of these adakitic rocks will be important for deciphering the tectonic evolution of the Tibetan Plateau.

Five genetic models have been proposed for adakites: (1) partial melting of subducting oceanic slab (Defant & Drummond, 1990); (2) crustal assimilation and fractional crystallization (AFC) processes from parental basaltic magmas (Castillo, Janney & Solidum, 1999); (3) partial melting of mafic rocks in the lower part of a thickened crust (Atherton & Petford, 1993; Xiong *et al.* 2003); (4) partial melting of a stalled (or dead) slab in the mantle (Pe-Piper & Piper, 1994; Defant *et al.* 2002; Mungall, 2002; Qu, Hou & Li, 2004) and (5) partial melting of delaminated or foundered lower crust (Kay & Kay, 1993; Xu *et al.* 2002; Gao *et al.* 2004; Wang *et al.* 2004*a*,*b*). The Qiangtang volcanic rocks have high Pb isotopic age-corrected ratios $(^{206}Pb/^{204}Pb)_i > 18$ (Table 3), similar to those of Mesozoic MORB and oceanic sediments in the West Pacific (Castillo, Pringle & Carlson, 1994; Shimoda *et al.* 1998). The adakitic lavas show a range of K_2O contents (2.97–3.81 wt %) (Table 1, Fig. 2), relatively high Th (12.7–18.9 ppm) and Rb (747–1289 ppm) contents, resulting in high Th/Ba (0.014–0.023), Th/U (3.0–6.2) and Rb/Ba (0.1–0.14, except three samples) ratios, relatively low Ba contents (747–1289 ppm) (Table 2) and no positive Sr anomalies (Table 2; Fig. 6b). These geochemical features exclude the first genetic hypothesis (Defant & Drummond, 1990), as well as the possibility that the adakitic rocks originated from a stalled slab in the mantle (Wang *et al.* 2006). Moreover, the low $\varepsilon_{Nd}(t)$ (−3.8 to −5.0) and high $(^{87}Sr/^{86}Sr)_i$ (0.7061–0.7077) features obviously distinguish them from adakites derived from partial melting of subducted oceanic slabs, such as those from Cook Island (Stern & Kilian, 1996), Adak Island (Kay, 1978) and Cerro Pampa (Kay, Ramos & Marquez, 1993), as these adakites have mid-ocean-ridge (MORB)-like Sr–Nd isotopic compositions (Gao *et al.* 2004). Geophysical evidence (Owens & Zandt, 1997; Tilmann *et al.* 2003) indicates that the N-trending subducted Indian plate and Tethyan oceanic slabs have not reached the southern boundary of the Qiangtang terrane (Bangong suture zone), suggesting that there was no subducted oceanic slab beneath the Qiangtang terrane when these adakitic rocks were generated. On a La/Yb v. La plot (Fig. 9), the adakitic rock compositions are more consistent with partial melting than a fractional crystallization trend, while their fairly high Mg no. (> 45 except for DGC–02) (Table 1) indicates that assimilation and fractional crystallization could not have produced the geochemical variation within the adakitic rocks (Castillo, Janney & Solidum, 1999). Moreover, there are no correlations between SiO_2, Rb and initial Sr isotopic compositions, which is inconsistent with the

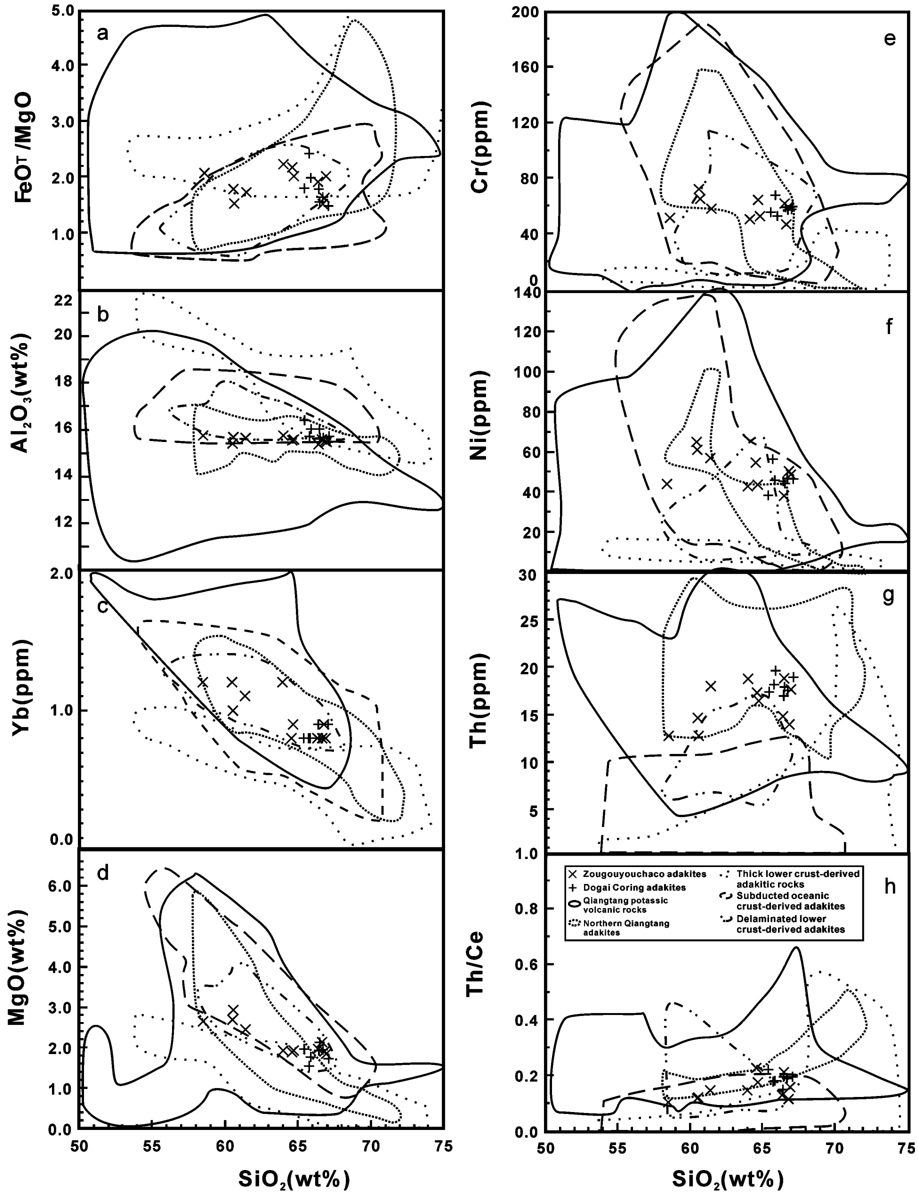

Figure 4. Harker variation diagrams showing the major and trace element variations of the Qiangtang adakites. Data for delaminated lower crust-derived adakitic rocks are constructed using the same data sources as Figure 3. The data for subducted oceanic crust-derived adakites are from Defant & Drummond (1990); Kay, Ramos & Marquez (1993); Drummond, Defant & Kepezhinskas (1996); Stern & Kilian (1996); Sajona *et al.* (2000); Defant *et al.* (2002); Aguillón-Robles *et al.* (2001); Martin *et al.* (2005). Data for thick lower crust-derived adakitic rocks are from Atherton & Petford (1993); Muir *et al.* (1995); Petford & Atherton (1996); Johnson, Barnes & Miller (1997) and Xiong *et al.* (2003). Other data sources are same as in Figure 2.

evolved isotopic compositions resulting from assimilation and fractional crystallization (AFC)-like processes in the lower crust (Gao *et al.* 2004). High Th/U is a feature of most Cenozoic volcanic rocks derived from the upper and lower crust and mantle within the Tibetan Plateau (McKenna & Walker, 1990; Turner *et al.* 1996; Miller *et al.* 1999). However, the Nd–Sr–Pb isotopic characteristics (Table 3; Figs 7, 8), the relatively high MgO, Cr and Ni contents as well as the low FeO_T/MgO ratios (Fig. 4; Table 1) of the adakitic rocks confirm that a mantle component may have played an important role in their petrogenesis. The Pb isotopic patterns (Fig. 8) highlight the problem of crustal contamination, and an old piece of continental crust in the amphibolite facies, depleted in U with respect to Th (high Th/U ratios) but undepleted in Rb (Taylor, Jones & Moorbath, 1984) as observed in this study (Table 2; Fig. 6b). Furthermore, sample SiO_2 contents are too high (60–68 wt %, except ZGYC–05) for magma produced directly by partial melting of mantle peridotite, which cannot yield melts more silicic than andesite or boninite (Green, 1980; Jahn & Zhang, 1984; Baker *et al.* 1995). Our samples also show geochemical characteristics distinct from the rhyolites derived from upper-crustal sources (McKenna & Walker, 1990; Wang *et al.* 2005). Therefore, lower-crustal melting is thought to

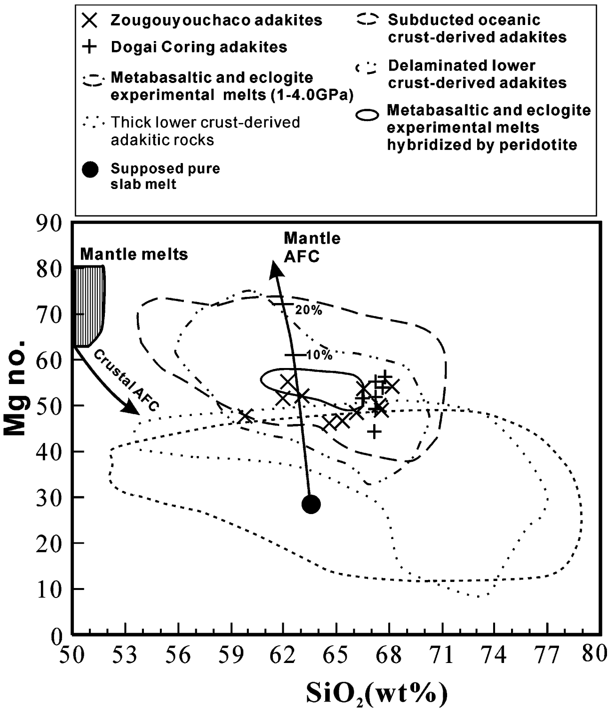

Figure 5. Mg no. v. SiO_2 diagram of Qiangtang adakites. Fields of delaminated lower crust-derived adakitic rocks, subducted oceanic crust-derived adakites and thick lower crust-derived adakitic rocks are constructed using the same data sources as those in Figure 3. The crustal AFC curve, mantle AFC curves and the supposed pure slab melts are after Stern & Killian (1996). The field of metabasaltic and eclogite experimental melts (1–4.0 GPa) is from the following: Rapp, Watson & Miller (1991); Rapp *et al.* (1999); Rapp, Xiao & Shimizu (2002); Sen & Dunn (1994); Rapp & Watson (1995); Prouteau *et al.* (1999); Skjerlie & Patino Douce (2002), and references therein. The field of metabasaltic and eclogite experimental melts hybridized with peridotite is after Rapp *et al.* (1999).

be the most likely interpretation for the origin of the Qiangtang volcanic rocks discussed here. Nevertheless, a remaining question is whether model (3) or model (5) is more reasonable.

If the adakitic rocks are derived directly from partial melting of mafic rocks in the lower crust, they should have relatively low MgO contents and Mg no. similar to the experimental melts of Rapp & Watson (1995). However, the adakitic volcanic rocks in this paper have relatively high MgO contents and Mg no. (Table 1; Figs 4d, 5), suggesting that pristine adakitic melts must have interacted to some extent with mantle peridotite (e.g. Kepezhinskas, Defant & Drummond, 1995; Stern & Kilian, 1996; Rapp *et al.* 1999; Smithies, 2000). In this case, the most likely scenario to explain the high MgO and Mg no. of the adakitic rocks seems to be foundering of the lower crust consisting of amphibole-bearing eclogitic materials, coinciding with dehydration melting of the delaminated crustal rocks in the hot mantle. Subsequently, the foundered crustal melts probably interacted with the surrounding mantle peridotite during emplacement.

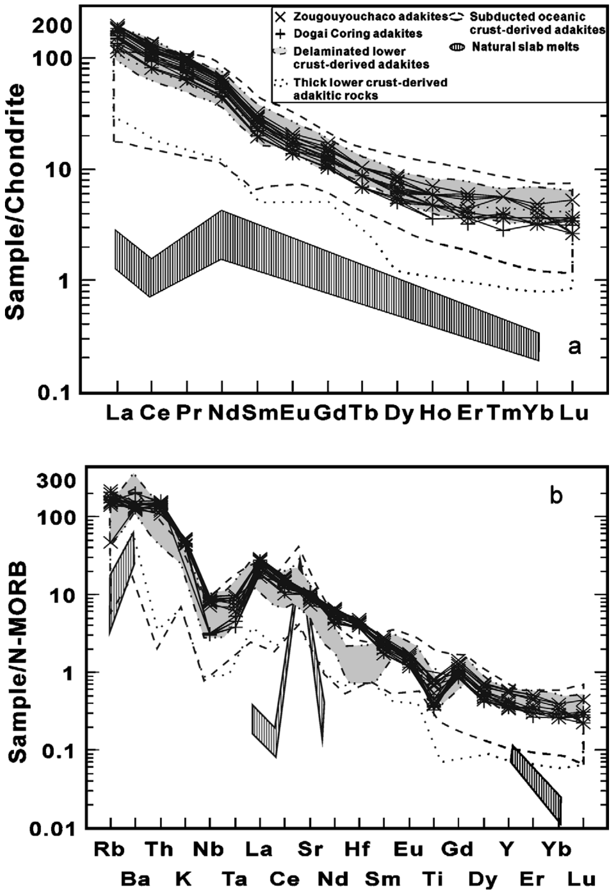

Figure 6. (a) Chondrite-normalized and (b) N-MORB-normalized spidergrams of Qiangtang adakitic volcanic rocks, northern Tibet. Normalized values are after Sun & McDonough (1989). The REE and trace elment data for delaminated lower crust-derived adakitic rocks, subducted oceanic crust-derived adakites, thick lower crust-derived adakites are constructed using the same data sources as those in Figure 3. The natural slab melt data are from Kepezhinskas, Defant & Drummond (1995) and Sorensen & Grossman (1989).

5.a.2. Source features

The highly enriched N-MORB normalized abundance patterns of trace elements for Qiangtang adakitic rocks (Fig. 6b) may suggest the existence of garnet as a residue in the mantle source beneath northern Tibet (Defant & Drummond, 1990; Drummond, Defant & Kepezhinskas, 1996; Defant & Kepezhinskas, 2001). The relative enrichment of Sr (up to 986 ppm) and the absence of significant Eu anomalies (Fig. 6) indicates either that plagioclase was not present in the source rock, or that it was completely consumed during melting. Nb partitions strongly into amphibole under equilibrium conditions (Pearce & Norry, 1979), whereas Ti partitions into rutile under hydrous mantle conditions (Tatsumi, 1986). However, both elements are strongly depleted in the Qiangtang adakitic rocks, which indicates that the source also has residual rutile and amphibole, and thus residues were most probably

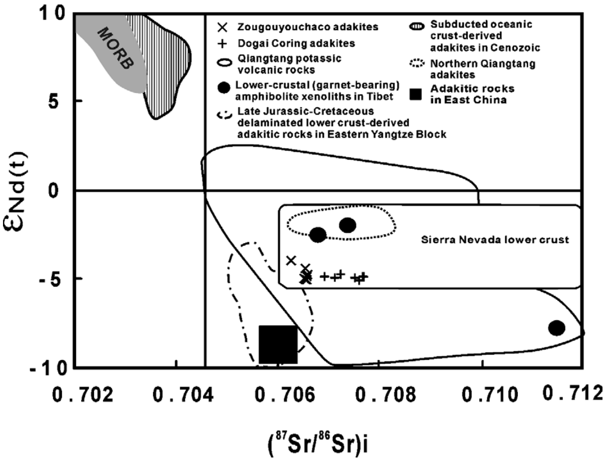

Figure 7. $\varepsilon_{Nd}(t)$ v. $(^{87}Sr/^{86}Sr)_i$ diagram of the adakitic volcanic rocks in Qiangtang terrane, northern Tibet. Data sources: Sierra Nevada lower crust from Ducea & Saleeby (1998); lower crust (garnet-bearing) amphibolite xenoliths in Tibet from Deng (1998); adakitic rocks in East China from Xu *et al.* (2002); subducted oceanic crust-derived adakites in Cenozoic after Defant *et al.* (1992), Kay, Ramos & Marquez (1993) and Sajona *et al.* (2000). MORB from Zindler & Hart (1986). Late Jurassic–Cretaceous delaminated lower crust-derived adakitic rocks in the eastern Yangtze block are from Wang *et al.* (2006). Qiangtang potassic volcanic rock data are from Pearce & Houjun (1993); Turner *et al.* (1996); Deng (1998); Ding *et al.* (1999, 2003); Yin *et al.* (2004); Williams *et al.* (2004). Northern Qiangtang adakitic rocks are from Lai, Qin & Li (2007).

hydrous amphibole-bearing and rutile-bearing eclogites (Mahoney *et al.* 1998).

5.a.3. Dynamic mechanism

Experimental studies (e.g. Rapp & Watson, 1995; Rapp *et al.* 1999; Rapp, Xiao & Shimizu, 2002; Rapp, Shimizu & Norman, 2003) indicate that mafic crustal rocks can melt to produce adakitic liquids at sufficient depths (> 40 km, that is, 1.2 GPa) for garnet to be stable within the residual assemblage (e.g. residues of garnet-amphibolite, amphibole-bearing eclogite and/or eclogite). The Qiangtang adakitic volcanic rocks display the typical adakitic affinities, such as high La/Yb, Sr/Y ratios and low Y and Yb contents (Table 2; Figs 3a, b, 6), implying that garnet was stable within the source residues when the adakitic magmas were segregated. Furthermore, rutile occurs at pressures higher than approximately 1.5 GPa (≥ 50 km crustal thickness), depending on H_2O content (2–5 wt %) and bulk composition (especially with bulk TiO_2: 1.72 wt % and K_2O: 1.43 wt %), during partial melting of hydrated basalt (Xiong, Adam & Green, 2005). Accordingly, the crustal thickness in the Qiangtang terrane must have been at least 50 km when the adakitic lavas were formed.

As a result of the collision between the Indian block and Asian block between Late Cretaceous and Early Cenozoic times (Yin & Harrison, 2000), the continental crust beneath Qiangtang was compressed and probably

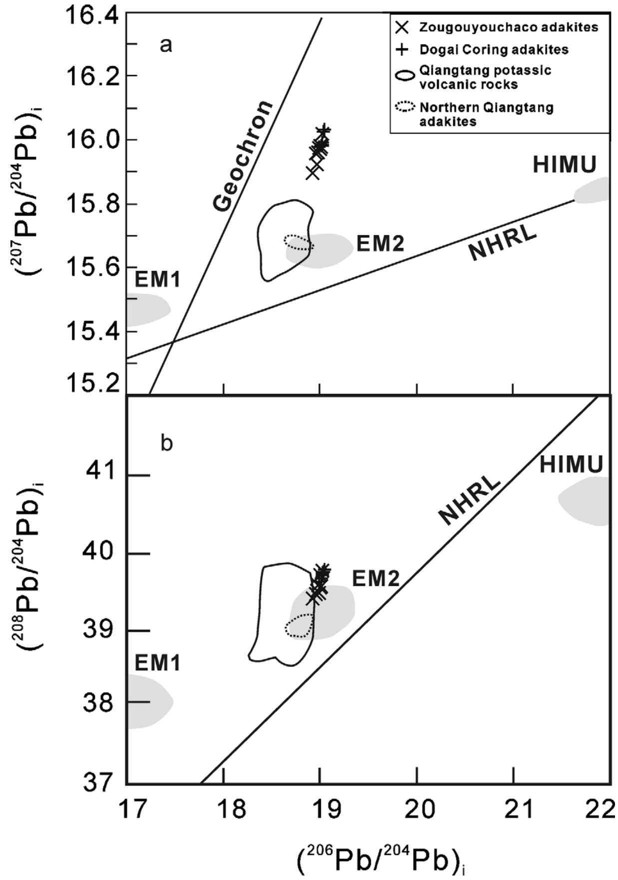

Figure 8. (a) $(^{207}Pb/^{204}Pb)_i$ and (b) $(^{208}Pb/^{204}Pb)_i$ v. $(^{206}Pb/^{204}Pb)_i$ diagrams of the adakitic rocks in Qiangtang terrane, northern Tibet. NHRL is from Hart (1984), Geochron (4.55 Ga) and the mantle end-members HIMU, EM1 and EM2 are after Zindler & Hart (1986). The Qiangtang potassic volcanic rocks are from Pearce & Houjun (1993); Turner *et al.* (1996); Deng (1998); Ding *et al.* (1999, 2003); Yin *et al.* (2004); Williams *et al.* (2004). Northern Qiangtang adakitic rocks are from Lai, Qin & Li (2007).

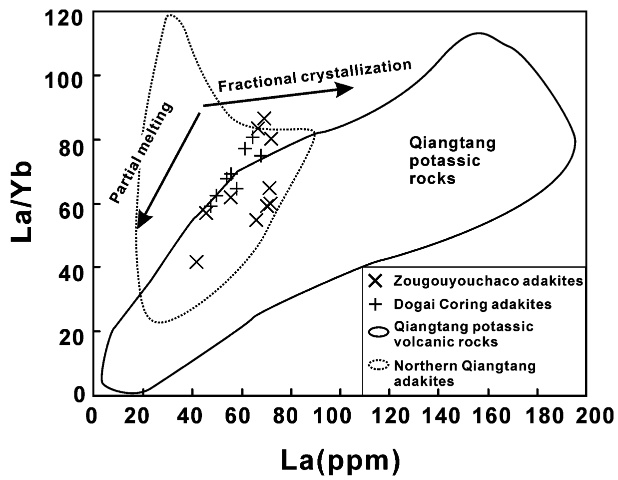

Figure 9. Plot of La/Yb v. La for the adakitic volcanic rocks in Qiangtang terrane, northern Tibet. The Qiangtang potassic volcanic rocks are from Pearce & Houjun (1993); Turner *et al.* (1996); Deng (1998); Ding *et al.* (1999, 2003); Yin *et al.* (2004); Williams *et al.* (2004); Turner *et al.* (1996); Tan, Pan & Xu (2000); Lai & Liu (2001); Lai *et al.* (2006). Northern Qiangtang adakitic rocks are from Lai, Qin & Li (2007).

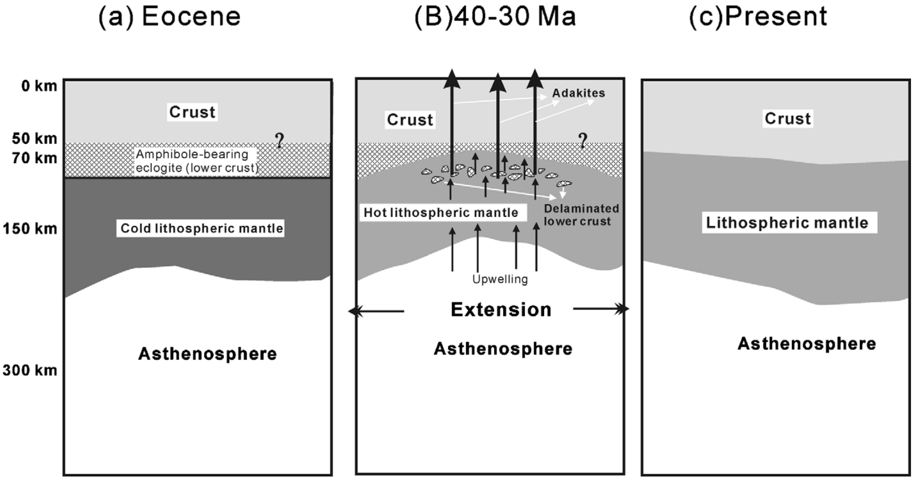

Figure 10. A suggested model to produce the adakitic volcanic rocks in Qiangtang via partial melting of delaminated lower crust from 40 to 30 Ma (modified from Xu *et al.* 2002). (a) The relatively cold lithospheric mantle and thick crust during Eocene times (Tapponnier *et al.* 2001). The thick lower crust is composed of amphibole-bearing eclogite. (b) The thick lower crust is removed through delamination or foundering due to density instability and has dived into the underlying hot lithospheric mantle, at the same time, the hot asthenospheric mantle wells up due to lithospheric delamination, extension and thinning. The adakitic melts are produced by dehydration melting of the delaminated lower crust (amphibole-bearing eclogite materials), which has been heated by the flux of heat from the hot lithospheric mantle and upwelling asthenosphere. The adakitic melts react with the surrounding mantle peridotite, enhancing their MgO, Cr and Ni contents. (c) The lithosphere framework beneath Qiangtang terrane at present (Wu, Xiao & Li, 1989).

over-thickened (> 70 km) in Eocene times (Tapponnier *et al.* 2001) (Fig. 10a); the increase in pressure and temperature would have transformed the basaltic lower crust into amphibolite-bearing eclogite in a thickened crust region (Austrheim, Erambert & Engvik, 1997) (Fig. 10a). Delamination is caused by the gabbro-eclogite transformation in the thickened continental lower crust (Sobolev & Babeyko, 2005). Once this transformation was complete, the eclogitized lower crust would delaminate and sink into the mantle due to its negative buoyancy (Kay & Kay, 1993; Gao *et al.* 2004). This would be balanced by an upwelling of hot asthenosphere material (Tilmann *et al.* 2003). Such an upward heat flow would provide a mechanism for heating the cold lithospheric mantle, delaminated crust and gradual erosion of remaining crust beneath Qiangtang terrane. After collision in the Early Cenozoic (Yin & Harrison, 2000), the release of stress led to extensional extension and thinning of the lithosphere beneath Qiangtang terrane at *c.* 40 Ma (Fig. 10b), allowing further upwelling flux from the asthenoshpere, and decompression melting of delaminated lower crust (amphibole-bearing eclogite materials) in hot mantle. Subsequently, significant chemical interaction will occur between mantle peridotite and the ascending crustal melt (Fig. 5), and produced the 40–30 Ma adakitic volcanic rocks in the Qiangtang terrane. However, amphibole-bearing and rutile-bearing eclogite would be left in the source, and cause strongly negative Nb and Ti anomalies.

6. Conclusions

(1) The high-K calc-alkaline volcanic rocks from Zougouyouchaco and Docai Coring in the Qiangtang terrane are adakites that were generated by partial melting of delaminated lower continental crust with a composition similar to the amphibole-bearing eclogitic materials beneath the Qiangtang terrane.

(2) The Nd–Sr isotopic signatures, their relatively high MgO, Mg no., Cr and Ni contents as well as low FeO_T/MgO ratios imply that the adakitic magmas include a significant mantle composition, and the existence of interaction between the delaminated lower crustal melts and the surrounding mantle peridotite.

Acknowledgements. We are grateful to T. F. Xiao, Y. Wang and J. Q. Liu for their helpful discussion and to the No. 2 Geology Team of Tibet for assistance with our fieldwork. We thank two anonymous reviewers, the editor David Pyle and the assistant editor Mrs Jane Holland for their constructive comments and suggestions that helped to improve the original manuscript. This work was supported by National Science Foundation of China (grant 40673029 and 40773020 to Liu, and 40634020 to Hu).

References

AGUILLÓN-ROBLES, A., CAIMUS, T., BELLON, H., MAURY, R. C., COTTON, J., BOURGOIS, J. & MICHAUD, F. 2001. Late Miocene adakites and Nb-enriched basalts from Vizcaino Peninsula, Mexico: indicators of East Pacific Rise subduction below southern Baja California. *Geology* **29**, 531–4.

ARNAUD, N. O., VIDAL, P., TAPPONNIER, P., MATTE, P. & DENG, W. M. 1992. The high K_2O volcanism of northwestern Tibet: Geochemistry and tectonic implications. *Earth and Planetary Science Letters* **111**, 351–67.

ATHERTON, M. P. & PETFORD, N. 1993. Generation of sodium-rich magmas from newly underplated basaltic crust. *Nature* **362**, 144–6.

AUSTRHEIM, H., ERAMBER, M. & ENGVIK, A. K. 1997. Processing of crust in the root of the Caledonian continental collision zone: the role of eclogitization. *Tectonophysics* **273**, 121–53.

BAKER, M. B., HISCHMANN, M. M., GHIORSO, M. S. & STOLPER, E. M. 1995. Compositions of near-solidus peridotite melt from experiments and thermodynamic calculations. *Nature* **375**, 308–11.

CASTILLO, P. R., JANNEY, P. E. & SOLIDUM, R. U. 1999. Petrology and geochemistry of Camiguin island, southern Philippines: insights to the source of adakites and other lavas in a complex arc setting. *Contributions to Mineralogy and Petrology* **134**, 33–51.

CASTILLO, P. R., PRINGLE, M. S. & CARLSON, R. W. 1994. East Mariana basin tholeiites: Cretaceous intraplate basalts or rift basalts related to the Ontong Java plume? *Earth and Planetary Science Letters* **123**, 139–54.

CHI, X. G., LI, C., JIN, W., LIU, S. & YANG, R. H. 1999. Temporal evolution of Cenozoic volcanism in northern Tibet and the uplifting of Qinhai-Tibet Plateau. *Geological Review* **45**, 978–85.

CHUNG, S. L., LIU, D. Y., JI, J. Q., CHU, M. F., LEE, H. Y., WEN, D. J., LO, C. H., LEE, T. Y., QIAN, Q. & ZHANG, Q. 2003. Adakites from continental collision zones: Melting of thickened lower crust beneath southern Tibet. *Geology* **31**, 1021–4.

CHUNG, S. L., LO, C. H., LEE, T. Y., ZHANG, Y. Q., XIE, Y. W., LI, X. H., WANG, K. L. & WANG, P. L. 1998. Diachronous uplift of the Tibetan plateau starting 40 Myr ago. *Nature* **394**, 769–73.

COLEMAN, M. & HODGES, K. 1995. Evidence for Tibetan plateau uplift before 14 Myr from a new minimum age for east-west extension. *Nature* **374**, 49–52.

COOPER, K. M., REID, M. R., DUNBAR, N. W. & MCINTOSH, W. C. 2002. Melt generation beneath northwestern Tibet: Constraints from ^{230}Th–^{238}U disequilibria. *Geochemistry, Geophysics, Geosystems* 10.1029/2002 GC000 332.

DEFANT, M. J. & DRUMMOND, M. S. 1990. Derivation of some modern arc magmas by melting of young subducted lithosphere. *Nature* **347**, 662–5.

DEFANT, M. J., JACKSON, T. E., DRUMMOND, M. S., DE BOER, J. Z., BELLON, H., FEIGENSON, M. D. *et al.* 1992. The geochemistry of young volcanism throughout western Panama and southeastern Costa Rica: an overview. *Journal of the Geological Society, London* **149**, 569–79.

DEFANT, M. J. & KEPEZHINSKAS, P. K. 2001. Evidence suggests slab melting in arc magmas. *EOS, Transactions American Geophysical Union* **82**, 65–9.

DEFANT, M. J., KEPEZHINSKAS, P., DEFANT, M. J., XU, J. F., KEPEZHINSKAS, P., WANG, Q., ZHANG, Q. & XIAO, L. 2002. Adakites: some variations on a theme. *Acta Petrologica Sinica* **18**(2), 129–42.

DENG, W. M. 1989. The Cenozoic volcanic rocks in north Ali area, Xizang. *Acta Petrologica Sinica* **3**, 1–11 (in Chinese with English abstract).

DENG, W. M. 1991. The geology, geochemistry and forming age of the shoshonitic volcanic rock in middle Kunlun orogenic belt. *Scientia Geologica Sinica* **3**, 201–13 (in Chinese with English abstract).

DENG, W. M. 1998. *Cenozoic intraplate volcnic rocks in the northern Qinghai–Xizang plateau*. Beijing: Geological Publishing House, 1–178.

DING, L., KAPP, P., YUE, Y. H. & LAI, Q. Z. 2007. Postcollisional calc-alkaline lavas and xenoliths from the southern Qiangtang terrane, central Tibet. *Earth and Planetary Science Letters* **254**, 28–38.

DING, L., KAPP, P., ZHONG, D. L. & DENG, W. M. 2003. Cenozoic volcanism in Tibet: Evidence from oceanic to continental subduction. *Journal of Petrology* **44**, 1833–65.

DING, L., ZHANG, J. J., ZHOU, Y., DENG, W. M., XU, R. H. & ZHONG, D. L. 1999. Tectonic implication on the lithosphere evolution of the Tibet Plateau: petrology and geochemistry of sodic and ultrapotassic volcanism in northern Tibet. *Acta Petrologica Sinica* **15**, 408–21.

DRUMMOND, M. S., DEFANT, M. J. & KEPEZHINSKAS, P. K. 1996. Petrogenesis of slab-derived trondhjemite–tonalite–dacite/adakite magmas. *Transactions Royal Society of Edinburgh, Earth Science* **87**, 205–15.

DUCEA, M. & SALEEBY, J. 1998. A case for delamination of the deep batholithic crust beneath the Sierra Nevada, California. *International Geology Review* **40**, 78–93.

GAO, S., RUDNICK, R. L., YUAN, H. L., LIU, X. M., LIU, Y. S., XU, W. L., LING, W. L., AYERS, J., WANG, X. C. & WANG, Q. H. 2004. Recycling lower continental crust in the North China craton. *Nature* **432**, 892–7.

GREEN, T. H. 1980. Island arc and continent-building magmatism: a review of petrogenetic models based on experimental petrology and geochemistry. *Tectonophysics* **63**, 367–85.

HACKER, B. R., GNOS, E., RATSCHBACHER, L., GROVE, M., MCWILLIAMS, M., SOBOLEV, S. V., JIANG, W. & WU, Z. 2000. Hot and dry deep crustal xenoliths from Tibet. *Science* **287**, 2463–6.

HART, S. R. 1984. A large-scale isotope anomaly in the Southern Hemisphere mantle. *Nature* **309**, 753–7.

HOU, Z. Q., GAO, Y. F., QU, M., RUI, Z. Y. & MAO, X. X. 2004. Origin of adakitic intrusives generated during mid-Miocene east–west extension in southern Tibet. *Earth and Planetary Science Letters* **220**, 139–55.

JAHN, B. M. & ZHANG, J. Q. 1984. Archean granulite gneisses from eastern Sino-Korean Province, China: rare earth geochemistry and tectonic implication. *Contributions to Mineralogy and Petrology* **85**, 224–43.

JOHNSON, K., BARNES, C. G. & MILLER, C. A. 1997. Petrology, geochemistry, and genesis of high-Al tonalite and trondhjemites of the Cornucopia stock, Blue Mountains, Northeastern Oregon. *Journal of Petrology* **38**, 1585–1611.

KAY, R. W. 1978. Aleutian magnesium andesites: melts from subducted Pacific oceanic slab. *Journal of Volcanology and Geothermal Research* **4**, 117–32.

KAY, R. W. & KAY, S. M. 1993. Delamination and delamination magmatism. *Tectonophysics* **219**, 177–89.

KAY, S. M., RAMOS, V. A. & MARQUEZ, M. 1993. Evidence in Cerro Pampa volcanic rocks of slab melting prior to ridge trench collision in southern South America. *Journal of Geology* **101**, 703–14.

KEPEZHINSKAS, P. K., DEFANT, M. J. & DRUMMOND, M. 1995. Na metasomatism in the island-arc mantle by slab melt–peridotite interaction: evidence from mantle interaction – evidence from mantle xenoliths in the north Kamchatka arc. *Journal of Petrology* **36**, 1505–27.

LAI, S. C. & LIU, C. Y. 2001. Enriched upper mantle and eclogitic lower crust in north Qiangtang, Qinghai–Tibet Plateau: petrological and geochemical evidence from the Cenozoic volcanic rocks. *Acta Petrologica Sinica* **17**, 459–68 (in Chinese with English abstract).

LAI, S. C., QIN, J. F. & LI, Y. F. 2007. Partial melting of thickened Tibetan Crust: Geochemical evidence from Cenozoic adakitic volcanic rocks. *International Geology Review* **49**, 357–73.

LAI, S., QIN, J., LI, Y. & LIU, X. 2006. Cenozoic volcanic rocks in the Belog Co area, Qiangtang, northern Tibet, China: petrochemical evidence for partial melting of the mantle–crust transition zone. *Geological Bulletin of China* **25**, 64–9.

LI, C., HUANG, X. P., MOU, S. Y. & CHI, X. G. 2006. ^{40}Ar–^{39}Ar dating for Kangtog formation volcanic rocks in Zougouyouchaco, Qiangtang, northern Tibet. *Geological Bulletin of China* **25**, 226–8 (in Chinese with English abstract).

LIANG, X. R., WANG, G. J., LI, X. H. & LIU, Y. 2003. Precise measurement of ^{143}Nd/^{144} Nd and Sm/Nd ratios using multiple-collectors inductively coupled plasma-mass spectrometer (M C-ICPMS). *Geochimica* **32**, 91–6.

LIU, J. Q. 1998. *Volcanoes in China*. Beijing: Science Press (in Chinese).

LUGMAIR, G. W. & HARTI, K. 1978. Lunar initial 143Nd/144Nd: differential evolution of the lunar crust and mantle. *Earth and Planetary Science Letters* **39**, 349–57.

MAHONEY, J. J., FREI, R., TEJADA, M. L. G., MO, X. X. & LEAT, P. T. 1998. Tracing the Indian ocean mantle domain through time: Isotopic results from old west Indian, east Tethyan and south Pacific seafloor. *Journal of Petrology* **39**, 1285–1306.

MARTIN, H., SMITHIES, R. H., RAPP, R., MOYEN, J. F. & CHAMPION, D. 2005. An overview of adakite, tonalite–trondhjemite–granodiorite (TTG), and sanukitoid: relationships and some implications for crustal evolution. *Lithos* **79**, 1–24.

MCKENNA, L. W. & WALKER, J. D. 1990. Geochemistry of crustally derived leucocratic igneous rocks from the Ulugh Muztagh area, northern Tibet, and their implications for the formation of the Tibetan Plateau. *Journal of Geophysical Research* **95**, 21483–502.

MILLER, C. R., SCHUSTER, U., KLOTZLI, W. F. & PURTSCHELLER, F. 1999. Post-collisional potassic and ultrapotassic magmatism in SW Tibet: Geochemical and Sr–Nd–Pb–O isotopic constraints for mantle source characteristics and petrogenesis. *Journal of Petrology* **40**, 1399–1424.

MUIR, R. J., WEAVER, S. D., BRADSHAW, J. D., EBY, G. N. & EVANS, J. A. 1995. Geochemistry of the Cretaceous Separation Point Batholith, New Zealand: granitoid magmas formed by melting of mafic lithosphere. *Journal of the Geological Society, London* **152**, 689–701.

MUNGALL, J. E. 2002. Roasting the mantle: slab melting and the genesis of major Au and Au-rich Cu deposits. *Geology* **30**, 915–18.

OWENS, T. J. & ZANDT, G. 1997. Implications of crustal property variations for models of Tibetan plateau evolution. *Nature* **387**, 37–43.

PEARCE, J. A. & HOUJUN, M. 1993. Volcanic rocks of the 1985 Tibet geotraverse; Lhasa to Golmud. *Philosophical Transactions of the Royal Society, London* **327**, 169–201.

PEARCE, J. A. & NORRY, M. J. 1979. Petrogenetic implications of Ti, Zr, Y and Nb variations in volcanic rocks. *Contributions to Mineralogy and Petrology* **69**, 33–47.

PE-PIPER, G. & PIPER, J. W. 1994. Miocene magnesian andesites and dacites, Evia, Greece: adakites associated with subducting slab detachment and extension. *Lithos* **31**, 125–40.

PETFORD, N. & ATHERTON, M. 1996. Na-rich partial melts from newly underplated basaltic crust: the Cordillera Blanca Batholith, Peru. *Journal of Petrology* **37**, 1491–1521.

PROUTEAU, G., SCAILLET, B., PICHAVANT, M. & MAURY, R. C. 1999. Fluid-present melting of ocean crust in subduction zones. *Geology* **27**, 1111–14.

QI, L., HU, J. & GREGOIRE, D. C. 2000. Determination of trace elements in granite by inductively coupled plasma mass spectrometry. *Talanta* **51**, 507–13.

QU, X. M., HOU, Z. Q. & LI, Y. G. 2004. Melt components derived from a subducted slab in late orogenic ore-bearing porphyries in the Gangdese copper belt, southern Tibetan plateau. *Lithos* **74**, 131–48.

RAPP, R. P., SHIMIZU, N. & NORMAN, M. D. 2003. Growth of early continental crust by partial melting of eclogite. *Nature* **425**, 605–9.

RAPP, R. P., SHIMIZU, N., NORMAN, M. D. & APPLEGATE, G. S. 1999. Reaction between slab-derived melts and peridotite in the mantle wedge: experimental constraints at 3.8 GPa. *Chemical Geology* **160**, 335–56.

RAPP, R. P. & WATSON, E. B. 1995. Dehydration melting of metabasalt at 8–32 kbar: implications for continental growth and crust–mantle recycling. *Journal of Petrology* **36**, 891–931.

RAPP, R. P., WATSON, E. B. & MILLER, C. F. 1991. Partial melting of amphibolite/eclogite and the origin of Archean trondhjemites and tonalites. *Precambrian Research* **51**, 1–25.

RAPP, R. P., XIAO, L. & SHIMIZU, N. 2002. Experimental constraints on the origin of potassium-rich adakite in east China. *Acta Petrologica Sinica* **18**, 293–311.

SAJONA, F. G., NAURY, R. C., PUBELLIRE, M., LETERRIER, J., BELLON, H. & COTTON, J. 2000. Magmatic source enrichment by slab-derived melts in young post-collision setting, central Mindanao (Philippines). *Lithos* **54**, 173–206.

SEN, C. & DUNN, T. 1994. Dehydration melting of a basaltic composition amphibolite at 1.5 and 2.0 GPa: implications for the origin of adakites. *Contributions to Mineralogy and Petrology* **117**, 394–409.

SHIMODA, G., TATSUMI, Y., NOHDA, S., ISHIZAKA, K. & JAHN, B. M. 1998. Setouchi high-Mg andesites revisited: Geochemical evidence for melting of subducting sediments. *Earth and Planetary Science Letters* **160**, 479–92.

SKJERLIE, K. P. & Patino DOUCE, A. E. 2002. The fluid-absent partial melting of a zoisite-bearing quartz eclogite from 1.0 to 3.2 GPa: implications for melting in thickened continental crust and for subduction-zone processes. *Journal of Petrology* **43**, 291–314.

SMITHIES, R. H. 2000. The Archaean tonalite–trondhjemite–granodiorite (TTG) series is not an analogue of Cenozoic adakite. *Earth and Planetary Science Letters* **182**, 115–25.

SOBOLEV, S. V. & BABEYKO, A. Y. 2005. What drives orogeny in the Andes? *Geology* **33**, 617–20.

SORENSEN, S. S. & GROSSMAN, J. N. 1989. Enrichment of trace elements in garnet amphibolites from a paleo-subduction zone: Catalina schist, southern California. *Geochimica et Cosmochimica Acta* **53**, 3155–77.

STEIGER, R. H. & JÄGER, E. 1977. Subcommission on geochronology; convention on the use of decay constants in geochronology and cosmochronology. *Earth and Planetary Science Letters* **36**, 359–62.

STERN, C. R. & KILIAN, R. 1996. Role of the subducted slab, mantle wedge and continental crust in the generation of adakites from the Austral volcanic zone. *Contributions to Mineralogy and Petrology* **123**, 263–81.

SUN, S. S. & MCDONOUGH, W. F. 1989. Chemical and isotopic systematics of oceanic basalts: implications for mantle composition and processes. In *Magmatism in the Ocean Basins* (eds A. D. Saunders & M. J. Norry), pp. 313–45. Geological Society of London, Special Publication no. 42.

TAN, F. W., PAN, G. T. & XU, Q. 2000. The uplift of Qinghai–Xizang Plateau and geochemical characteristics of Cenozoic volcanic rocks from the center of Qiangtang, Xizang. *Acta Petrologica et Mineralogica* **19**, 121–30 (in Chinese with English abstract).

TAPPONNIER, P., XU, Z. Q., ROGER, F., MEYER, B., ARNAUD, N., WITTLINGER, G. & YANH, J. S. 2001. Oblique stepwise rise and growth of the Tibet plateau. *Science* **294**, 1671–77.

TATSUMI, Y. 1986. Chemical characteristics of fluid phase released from a subduction lithosphere and origin of arc magma: evidence from high-pressure experiments and natural rocks. *Journal of Volcanology and Geothermal Research* **29**, 293–309.

TAYLOR, P. N., JONES, N. W. & MOORBATH, S. 1984. Isotopic assessment of relative contributions from crust and mantle sources to the magma genesis of Precambrian granitoid rocks. *Philosophical Transactions of the Royal Society of London* **310**, 605–25.

TILMANN, F., NI, J. & INDEPTH III SEISMIC TEAM,. 2003. Seismic imaging of the downwelling Indian lithosphere beneath central Tibet. *Science* **300**, 1424–7.

TURNER, S. P., ARNAUD, N., LIU, J., RODGERS, N., HAWKESWORTH, C., HARRIS, N., KELLEY, S., VAN CALSTEREN, P. & DENG, W. 1996. Post-collision, shoshonitic volcanism on the Tibetan Plateau: implications for convective thinning of the lithosphere and the source of ocean island basalts. *Journal of Petrology* **37**, 45–71.

WANG, Q., MCDERMOTT, F., XU, J. F., BELLON, H. & ZHU, Y. T. 2005. Cenozoic K-rich adakitic volcanic rocks in the Hohxil area, northern Tibet: Lower crustal melting in an intra-continental setting. *Geology* **33**, 465–8.

WANG, Q., XU, J. F., JIAN, P., BAO, Z. W., ZHAO, Z. H., LI, C. F., XIONG, X. L. & MA, J. L. 2006. Petrogenesis of adakitic porphyries in an extensional tectonic setting, Dexing, South China: Implications for the genesis of porphyry copper mineralization. *Journal of Petrology* **47**, 119–47.

WANG, Q., XU, J. F., ZHAO, Z. H., BAO, Z. W., XU, W. & XIONG, X. L. 2004*a*. Cretaceous high-potassium intrusive rocks in the Yueshan–Hongzhen area of east China: adakites in an extensional tectonic regime within a continent. *Geochemical Journal* **38**, 417–34.

WANG, Q., ZHAO, Z. H., BAO, Z W., XU, J. F., LIU, W., LI, C. F. *et al.* 2004*b*. Geochemistry and petrogenesis of the Tongshankou and Yinzu adakitic intrusive rocks and the associated porphyry copper–molybdenum mineralization in southeast Hubei, east China. *Resource Geology* **54**, 137–52.

WILLIAMS, H. M., TURNER, S. P., KELLEY, S. & HARRIS, N. 2001. Age and composition of dikes in Southern Tibet: new constraints on the timing of east–west extension and its relationship to postcollisional volcanism. *Geology* **29**, 339–42.

WILLIAMS, H. M., TURNER, S. P., PEARCE, J. A., KELLEY, S. P. & HARRIS, N. B. W. 2004. Nature of the source regions for post-collisional, potassic magmatism in southern and northern Tibet from geochemical variations and inverse trace element modeling. *Journal of Petrology* **45**, 555–607.

WU, G. J., XIAO, X. C. & LI, T. D. 1989. The Yadong-Golmud geoscience section on the Qinghai-Tibet Plateau. *Acta Geologica Sinica* **4**, 285–96 (in Chinese with English abstract).

XIONG, X. L., ADAM, J. & GREEN, T. H. 2005. Rutile stability and rutile/melt HFSE partitioning during partial melting of hydrous basalt: implications for TTG genesis. *Chemical Geology* **218**, 339–59.

XIONG, X. L., LI, X. H., XU, J. F., LI, W. X., ZHAO, Z. H. & WANG, Q. 2003. Extremely high-Na adakite-like magmas derived from alkali-rich basaltic underplate: the Late Cretaceous Zhantang andesites in the Huichang Basin, SE China. *Geochemical Journal* **37**, 233–52.

XU, J. F., SHINJIO, R., DEFANT, M. J., WANG, Q. & RAPP, R. P. 2002. Origin of Mesozoic adakitic intrusive rocks in the Ningzhen area of east China: partial melting of delaminated lower continental crust? *Geology* **32**, 1111–14.

YIN, A. & HARRISON, T. M. 2000. Geologic evolution of the Himalayan–Tibetan orogen. *Annual Review of Earth and Planetary Sciences* **28**, 211–80.

YIN, H. S., LIN, J. H, LI, B. H., ZHAO, B., SHI, Z. Q., HUANG, J. J, SUN, C. M., LAI, S. C., ZHU, Y. T. & ZHAO, X. X. 2004. *High-K calc-alkaline volcanic rocks and crust–mantle interaction in Qinghai–Xizang plateau*. Beijing: Geological Publishing House, 1–95 (in Chinese).

ZINDLER, A. & HART, S. R. 1986. Chemical geodynamics. *Annual Review of Earth and Planetary Sciences* **14**, 493–571.